

Human Lung Air Spaces: Potential for MR Imaging with Hyperpolarized He-3¹

James R. MacFall, PhD
H. Cecil Charles, PhD
Robert D. Black, PhD
Hunter Middleton, PhD
John C. Swartz, PhD
Brian Saam, PhD
Bastiaan Driehuys, PhD
Christopher Erickson, BS
William Happer, PhD
Gordon D. Cates, PhD
G. Allan Johnson, PhD
Carl E. Ravin, MD

Two healthy volunteers who had inhaled approximately 0.75 L of laser-polarized helium-3 gas underwent magnetic resonance imaging at 1.5 T with fast gradient-echo pulse sequences and small flip angles (<10°). Thick-section (20 mm) coronal images, time-course data (30 images collected every 1.8 seconds), and thin-section (6 mm) images were acquired. Subjects were able to breathe the gas (12% polarization) without difficulty. Thick-section images were of good quality and had a signal-to-noise ratio (S/N) of 32:1 near the surface coil and 16:1 farther away. The time images showed regional differences, which indicated potential value for quantitation. High-resolution images showed greater detail and a S/N of approximately 6:1.

Index terms: Lung, MR, 60.12143 • Magnetic resonance (MR), contrast enhancement, 60.12143 • Magnetic resonance (MR), nuclei other than H, 60.12147

Radiology 1996; 200:553-558

¹From the Departments of Radiology (J.R.M., H.C.C., R.D.B., G.A.J., C.E.R.) and Physics (J.C.S.), Duke University Medical Center, Bryan Research Bldg, Rm 161C, Research Dr, Durham, NC 27710; and the Department of Physics, Princeton University, Princeton, NJ (H.M., B.S., B.D., C.E., W.H., G.D.C.). Received February 12, 1996; revision requested March 13; revision received March 26; accepted April 1. Supported in part by National Institutes of Health grant P41-RR05959, National Science Foundation grant CDR-8622201, Air Force Office of Scientific Research grant F49620-92-J-0211, Advanced Research Projects Agency grant DAMD17-94-J-4469, and Army Research Office DAAH04-94-0204, and by GE Medical Systems. Address reprint requests to J.R.M.
© RSNA, 1996

CLINICAL magnetic resonance (MR) imaging provides a map of the distribution of hydrogen-1 density in human subjects, mainly in water and fat. Contrast is also provided by the relaxation values (T₁, T₂) of the H-1 in the tissue and the pulse sequence selected (repetition time, echo time). The success of MR imaging has depended in part on the high concentration of H-1 in tissue. The density of water vapor is very low (on the order of 10⁻⁴ of the density of water in tissue). MR imaging of the gas spaces in the lungs and the movement of gases (ventilation) has seemed technically unfeasible, since the signal from such sources would also be 10⁻⁴ of the signal from tissue and thus would be too low to image successfully.

MR imaging of lung gas space is also challenged by poor magnetic-field homogeneity due to many tissue-air interfaces and to the presence of artifacts caused by physiologic motion (cardiac, respiratory). Many MR imaging systems include techniques to reduce or control for motion artifacts. Also, the use of a very short echo time can reduce signal loss due to the magnetic inhomogeneities. The low gas density in lung air spaces, however, has continued to be a problem with conventional MR imaging.

MR imaging generally has low sensitivity because only a very small fraction of H-1 spins are polarized by the applied magnetic field. Typically, spins in a 1.5-T magnetic field will experience only a 10⁻⁶ polarization (predominance of spins populating the low-energy spin state vs the high-energy spin state).

Dramatically higher polarization values have been achieved with noble gases such as xenon-129 and helium-3 by using optical pumping with lasers, rather than a magnetic field, to create the population difference in the spin states (1,2). With this method, polarizations exceeding 50% can be developed that offer a possible 10⁵-10⁶ signal enhancement factor. Because the signal is a function of the polarization and the density, the result is a potential factor of 10²-10³ signal enhancement. Other considerations related to the difference in the resonant frequency of He-3 or Xe-129 and H-1 can further reduce the potential signal enhancement to between a factor of 10 and 100. Such images have been obtained by using hyperpolarized He-3 in guinea pig lungs (2). In this study, we evaluated the methods and results of obtaining hy-

perpolarized He-3 images in human lung gas spaces.

Materials and Methods

Gas preparation.—He-3 gas was hyperpolarized by means of spin-exchange collisions with optically pumped rubidium atoms (3), as has been described in detail previously (2). Briefly, research-grade He-3 gas is purchased commercially and transferred to a 150-mL cylindric aluminosilicate glass chamber at 10 atm along with 70 mm Hg of nitrogen-2 and 0.1 g of rubidium metal. The container is heated to 180°C and exposed to 100 W of circularly polarized irradiation from a diode laser array aligned to illuminate the entire volume along the axis of the cylinder. The laser is tuned to the 795-nm D1 resonance of rubidium. The laser induces electronic spin polarization of the rubidium, and this polarization is transferred to the He-3 by means of collisional spin exchange.

The apparatus was aligned with the 10-G fringe field of a 1.5-T imaging magnet. This allowed the polarization buildup to be monitored with a low-field pulsed (nonimaging) nuclear MR detector. After 10-12 hours of optical pumping, polarization levels of between 5% and 15% were achieved. Subsequently the container was cooled to room temperature, which caused most of the rubidium to be deposited on the inner surface of the container. Residual rubidium vapor concentration was 10¹⁰ atoms per milliliter. The T₁ value of the polarized He-3 was at least several hours in the high-pressure glass container.

MR imaging.—Imaging was performed at 1.5 T with a whole-body, commercially available MR imaging unit (Signa, revision 5.3; GE Medical Systems, Milwaukee, Wis) equipped with the spectroscopy accessory. Magnitude images were acquired with a gradient-echo pulse sequence. Normally, such a pulse sequence uses a narrow-band receiver tuned to the Larmor frequency for protons at 1.5 T. The pulse sequence was modified with the manufacturer's research software to use the broad-band receiver that is supplied with its spectroscopic imaging product and to adjust the gradient strengths for the difference in gyromagnetic ratio between He-3 (3,459.31 Hz/G) and H-1 (4,257.26 Hz/G). Thus the same sequence could be used to image at H-1 (63.87-MHz) and He-3 (48.65-MHz) frequencies.

A unique feature of imaging with hyperpolarized gas is that there is no need to include spin T1 recovery considerations in the choice of repetition time because there is no recovery of the hyperpolarization in the magnetic field. Thus, a repetition time was chosen that was as short as possible for the readout bandwidth, and an echo time was chosen that was as short as possible with the available gradient strength (1 G/cm, 600-second rise time). Typical operating parameters included coronal orientation, 128×256 matrix, 32-cm field of view, and one signal acquired.

Three examinations were performed. The first, thick-section imaging, was performed with 20-mm section thickness, acquisition of three sections, 14.9/3.3 (repetition time msec/echo time msec), 6° flip angle, and plus or minus 4-kHz bandwidth. Acquisition of the three sections was repeated five times during a 28-second breath hold.

Dynamic imaging was performed with 20-mm section thickness, 7.0/2, 3° flip angle, and plus or minus 16-kHz bandwidth. Thirty images were collected for each of two sections in an interleaved fashion during a period of 54 seconds. The time necessary to obtain an individual image was 0.9 seconds, and the time that elapsed between acquisition of consecutive images for a given section was 1.8 seconds. The subject began shallow breathing after approximately 20 seconds of breath holding while the imaging continued.

Thin-section imaging was performed with a 6-mm section thickness, acquisition of 30 sections, 9.5/3.0, 8° flip angle, and plus or minus 16-kHz bandwidth. The sections were obtained in two passes: The odd-numbered sections were collected in the first pass, and the even-numbered sections were collected in the second pass. The total acquisition time was 36 seconds during a breath hold.

Because the conventional coils for the MR imaging system are tuned for H-1 imaging, an octagonal transmit-receive surface coil 26 cm in diameter (center of conductor) was constructed for the He-3 imaging as shown in Figure 1. The coil was fabricated of 1.25-cm-wide copper foil tape (3M, St Paul, Minn) on a 0.635-cm-thick acrylic substrate with the capacitance (high Q, ceramic capacitors; Dielectric Laboratories, Cazenovia, NJ) distributed on each leg of the structure (eight capacitors total, 120 pF per capacitor). This coil, when loaded with a subject, had a quality factor (Q_L) of 40. The matching network was an element design (4). A standard H-1 frequency preamplifier (GE Medical Systems) with a noise figure of less than 0.5 dB was capacitively retuned for use at the He-3 frequency, and a transmit-receive switch was constructed with use of a lumped

element "quarter wave" design (4).

The choice of flip angle in hyperpolarized gas imaging is similar to that in conventional imaging of objects with extremely long T1 values. Because the longitudinal magnetization does not recover to the hyperpolarized level, small flip angles must be used to leave sufficient magnetization for the typically 128 or 256 radio-frequency pulses used in a pulse sequence. Ideally, for a single image, the flip angle would slowly increase during imaging, so that a constant transverse magnetization would be created from the gradually declining longitudinal magnetization. For the present studies, a simpler scheme was used that incorporated a constant radio-frequency flip angle, under the requirement that the transverse magnetization near the end of data acquisition for an image should be reduced by no more than 50% of the initial transverse magnetization. The fraction of magnetization left after n radio-frequency pulses of flip angle α is $\cos^n(\alpha)$; therefore, when n equals 128 pulses and α equals 6° the initial magnetization is reduced by about 50%.

For H-1 imaging, flip angles conventionally have been scaled from the amplitude of the radio-frequency power that corresponds to a 90° flip angle as determined with a preimaging procedure. During this procedure, a 90° pulse should create the maximum signal as long as the repetition time is long enough to allow complete recovery of magnetization. This preimaging procedure cannot be performed in the same manner as a breath hold of polarized He-3, because pulses near 90° remove magnetization that does not recover and hence invalidate the preimaging assumptions. Thus, an approximate determination of the flip angle for the coil was made before human imaging began by using a high-pressure (approximately 10 atm) He-3 nonhyperpolarized phantom, which produces a small but detectable signal, placed at the center of the coil. The coil was loaded with a saline bolus to mimic a human chest. Transmit levels for 90° and 180° pulses were determined with this phantom and were used to calculate the appropriate level for the hyperpolarized gas examinations. Note that because a transmit-receive surface coil was used, the flip-angle calibration refers to the center of the coil. The value of the flip angle away from the center of a circular surface coil falls slowly along the axis for small distances. It reaches 70% of the central value at a distance of one-half the radius and falls to 35% of the value at a distance of 1 radius (5).

Subjects and imaging procedure.—Two healthy male volunteers, aged 38 and 46 years, underwent MR imaging at Duke University Medical Center. The

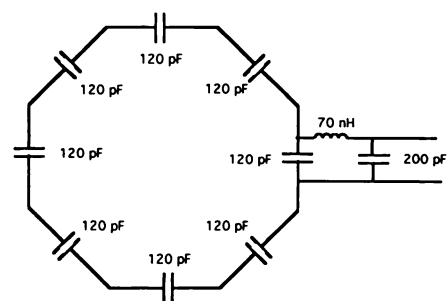


Figure 1. Diagram of the transmit-receive surface coil used for the He-3 imaging. The octagonal section was constructed with 1.25-cm-wide copper foil tape on 0.635-cm-thick acrylic substrate. The coil diameter is 26 cm. pF = picofarad, nH = nanohenry.

study protocol was approved by the institutional review board, and informed consent was obtained. The subject's heart rate and partial pressure of oxygen were monitored during imaging (Omni-Trak; In Vivo Research, Orlando, Fla). Each subject first underwent conventional H-1 MR imaging so that the region of interest could be located and the general anatomic structures could be visualized. After the MR system was prepared for He-3 imaging, the He-3 gas was passed through a 0.2-m filter (Gelman Sciences, Ann Arbor, Mich) to ensure complete removal of rubidium particles from the gas stream. A gas sample from a similarly polarized cell (obtained without the filter) was analyzed with a residual gas analyzer (Dataquad DAQ 3.2; SpectraMass, Congelton, Cheshire, England) and was found to have no detectable level of rubidium. The filtered gas was collected in a conventional plastic bag (approximately 1.2 L of He-3) to which a plastic tube and hand-operated valve were attached.

The bag was delivered to the subject in the magnet, and the subject was instructed to open the valve, inhale the gas through the tube, and hold his breath as long as he could. We estimated that approximately 0.75 L of gas actually reached the imaging volume. The subject also had a "squeeze bulb" that actuated a signal audible to the MR operator. For the thick-section and thin-section examinations, the subject actuated the signal when he had completely inhaled the gas. For the dynamic examination, the subject actuated the signal as he began to inhale the gas. Imaging was started when the signal was heard by the operator.

The thick-section and dynamic examinations were performed with one volunteer. The thin-section examination was performed with the second volunteer.

Image analysis.—The signal-to-noise ratio (S/N) of images was calculated for the different examinations by using the display features of the MR system (a cir-

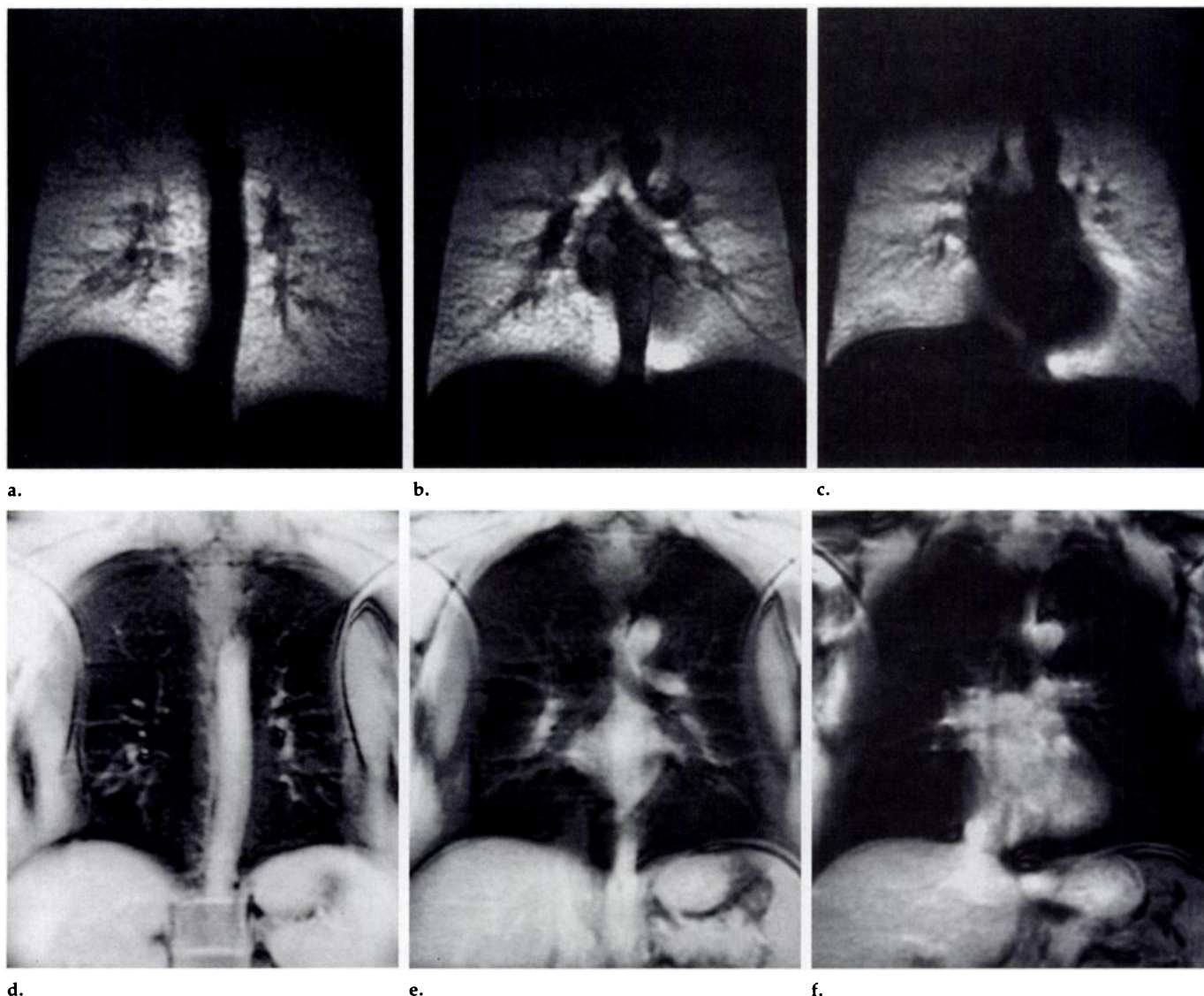


Figure 2. (a–c) Thick-section (20 mm) coronal He-3 images and (d–f) corresponding H-1 images of the lungs in a healthy human volunteer. The falloff in signal intensity in the apex of the lungs in the He-3 images is due to the position and limited receptivity (26 cm) of the surface coil. The signal intensity on the left and right sides near the edges in d–f is an aliasing artifact from the arms and shoulders, which were outside the field of view.

cular cursor superimposed on the image) to define a region of interest. A region of interest of 98 mm² was used to determine the average image intensity in a region of the lung field judged to represent “average” features. Also, the standard deviation in a similar region of interest positioned outside the subject and that consisted of noise was used to approximate the image noise (the “air” noise). The S/N was calculated as the ratio of the average region-of-interest signal intensity to the measured air noise. The S/Ns were then corrected by a factor of 0.65 to account for use of air noise, which resulted in underestimation of the true standard deviation (6).

Results

Thick-section imaging.—The subject reported no discomfort during the He-3 breath hold except for a mild tickling

sensation at the back of his throat at the end of the breath hold. His Po₂ remained within normal limits for breath holding and his heart rate increased slightly, but both indicators returned to normal after imaging.

The gas processing reached a polarization value of 13%. The signal saturated the preamplifier for the first two repetitions of the sequence and caused strong image artifacts that made the images unusable. Representative thick-section He-3 images corresponding to the third repetition are shown along with the corresponding H-1 images in Figure 2. The S/N for an average-intensity region was on the order of 32:1 in the most anterior image in Figure 2 and decreased to approximately 16:1 in the most posterior image for data acquired in the middle of the acquisition (third repetition).

Dynamic imaging.—The subject re-

ported no discomfort or difficulty in breathing the He-3, and the monitored heart rate and Po₂ changes were unremarkable. Gas polarization for this examination was 5%. A representative sequence of images is shown in Figure 3. The S/N for a representative region on the earliest image was approximately 26:1.

Figure 4 is a graph of image intensity as a function of time (image number) for three regions of interest positioned near the apex, middle, and bottom (near the diaphragm) of the lung, respectively, in the most anterior image series.

Thin-section imaging.—The subject reported no discomfort or ill effects after inhaling the He-3. There were no notable changes in his heart rate or Po₂. A representative image is shown in Figure 5. The gas polarization for this examination was 7%. The S/N for the first-pass

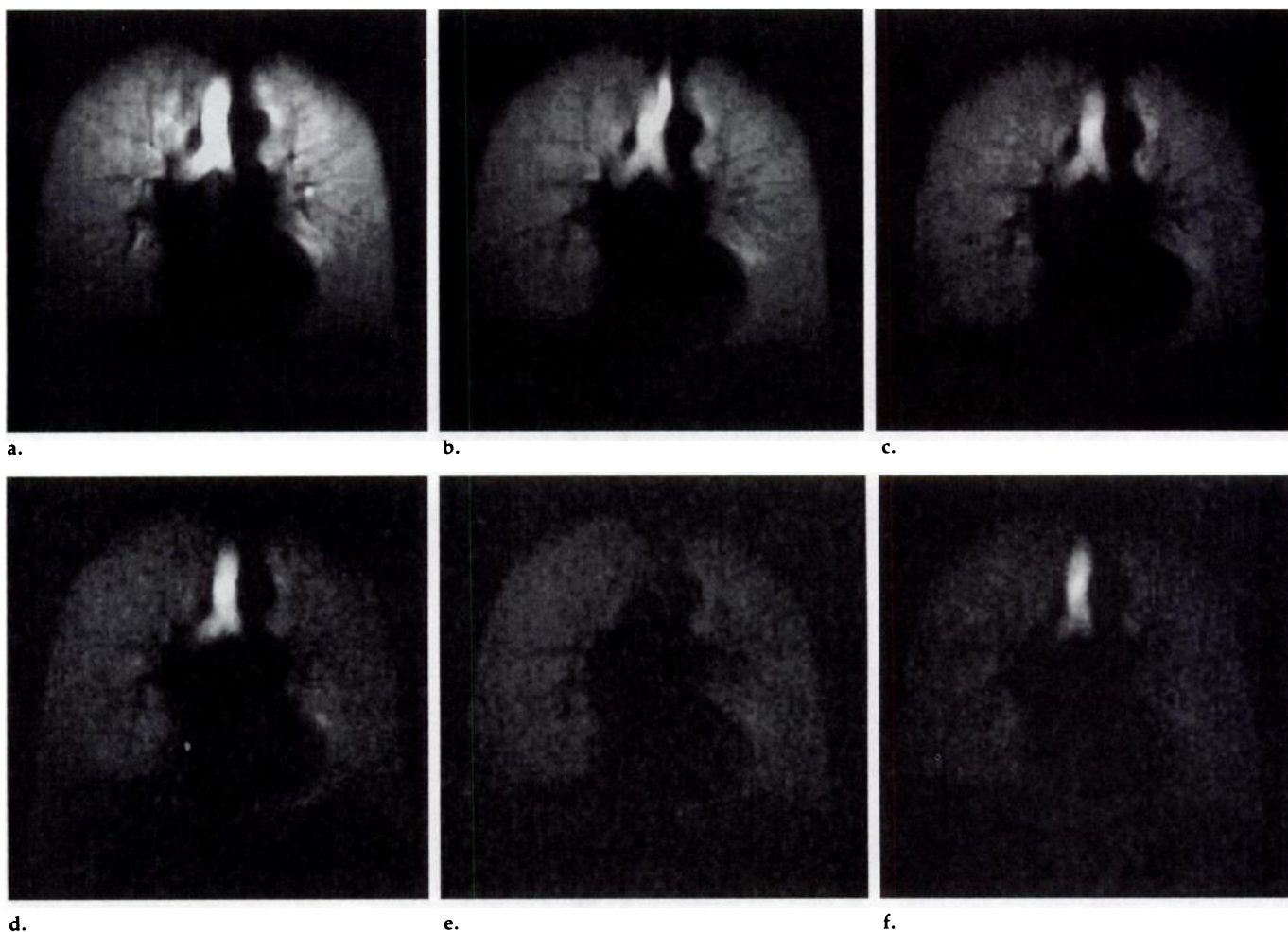


Figure 3. He-3 images selected from a dynamic examination (30 images obtained at 1.8-second intervals) of the distribution of He-3 in the lungs of a healthy volunteer. Acquisition of these images was separated by 3.6 seconds. A reduction in signal intensity due to repetitive imaging of the same section during a breath hold can be seen in (a–d) the initial images. The He-3 signal intensity in the trachea (e) disappears when the subject begins shallow breathing of room air and then (f) reappears during exhalation.

(odd-numbered) images in the anterior region was on the order of 6:1. For the second-pass (even-numbered) sections, the S/N was a factor of nearly one-third less.

Discussion

These results show that very good quality images of the distribution of He-3 in the lungs of a human subject can be obtained with approximately 0.75 L of hyperpolarized He-3 (approximately 8% polarized) and with a minimally modified commercial 1.5-T MR imaging system. The pulse sequence and coils were of conventional design, and their use was well within the capability of most systems and the abilities of most researchers. Typically, multiple acquisitions were made in a given location; therefore, even better S/N could be obtained with use of larger flip angles and a single acquisition.

Thick-section imaging.—The nonuniformity and falloff in signal intensity toward the edges (especially in the apices) was consistent with the position of

the surface transmit-receive coil, and the reduction in depth of intensity was also to be expected. The actual anatomic resolution appeared to approach that determined by means of calculated pixel dimension (1.25×2.5 mm) as shown by the sharp cutoff of signal intensity at the left and right edges of the lung and at the diaphragm. The indentations into the lungs by the ribs were also remarkable. In addition, the paths of blood vessels appeared as tracks of low intensity, indicating that the He-3 was not taken up by the blood in any large quantity.

The signal intensity that appeared outside the lung in the mediastinal spaces (Fig 2c, center) was an artifact. This artifact was caused by minor saturation of the receiver by the large initial signal at the lowest phase-encoding value in the acquisition and was not thought to represent any penetration of gas into the mediastinal and pleural spaces. The saturation was due to the difficulty of precisely setting the gain of the receiver as described earlier. The subsequent repetitions had a lower sig-

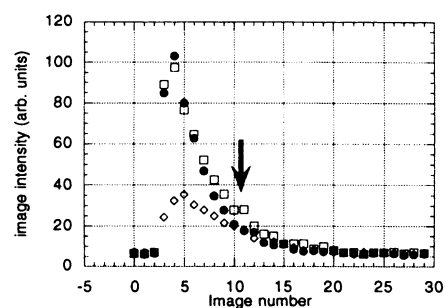


Figure 4. Graph of He-3 signal intensity (arbitrary [arb.] units) as a function of image number (0.9 second per image, 1.8-second interval) for three regions of interest (area = 98 mm^2) in the lung of a healthy volunteer. The regions of interest are at the apex (\square), middle (\bullet), and bottom (\diamond) of the left lung. The subject began shallow breathing of room air between the 10th and 11th image (arrow).

nal intensity and no noticeable exterior signal. Figure 2c illustrates this effect at the second repetition of the image. Figure 2a and 2e (fifth repetitions) show that the effect is not present later when

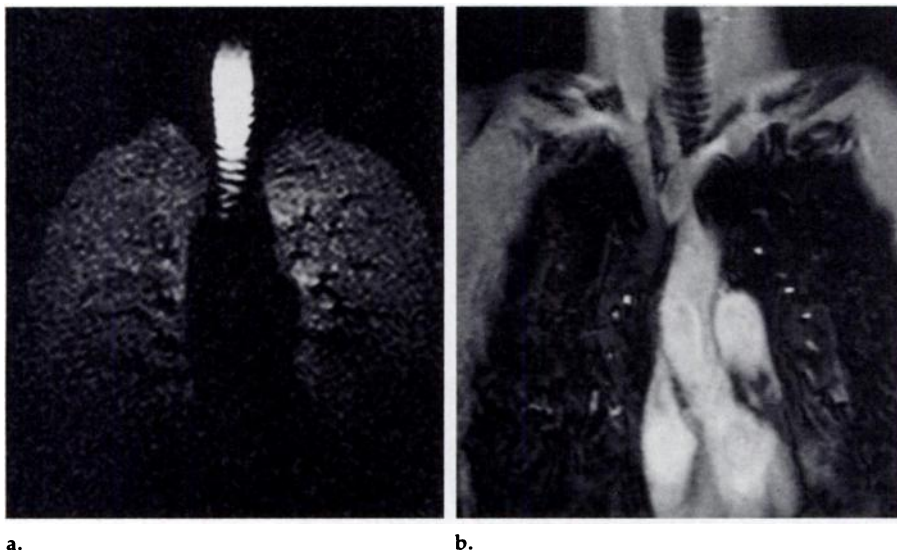


Figure 5. (a) Thin-section (6 mm) coronal He-3 image of the lung in a healthy volunteer was obtained at a position through the heart. The falloff in signal intensity toward the bottom of the lung is due to the position and limited receptivity (26 cm) of the surface coil. (b) H-1 image of the same region was obtained to help orientation and identification of the anatomic structures.

the signal intensities are decreased. The initial S/N, calculated on the basis of the flip angle prescribed, should be about a factor of 4 higher than that of the third repetition, because each image consumes about half of the available magnetization.

Dynamic imaging.—The coil was positioned more toward the head in this examination than in the thick-section examination. This new position provided better image quality in the apex of the lung but reduced signal intensity near the diaphragm. Use of a reduced flip angle helped preserve the signal intensity throughout the examination, even though the S/N was reduced from the previous examination, because the bandwidth was wider, the polarization was lower, and the flip angle was smaller.

The graph in Figure 4 shows the typical regional dynamics of filling the lungs with gas and exhaling the gas. It also shows the effects of the loss of polarization during the imaging process. Note the delayed peak of the lower part of the lung compared with the other regions. The image intensity was reduced by about 28% after each image was obtained during breath hold and was reduced at a lower rate thereafter. The expectation had been that the signal intensity would be reduced more rapidly during shallow breathing, owing to simple dilution of the He-3 with air; however, the lower-than-expected reduction may be evidence of more complicated gas dynamics that involve inflow of He-3 from unimaged regions of the lung. He-3 from unimaged regions would be at full polarization and would thus slow the loss of image signal intensity. Therefore, although the

dynamics appear to be complicated, the fact that the different regions showed different rates of filling and clearance indicates that quantitation of the MR-image time sequences may allow quantitation of regional ventilation.

The series in Figure 3 shows the disappearance of signal intensity in the trachea when the subject began to breathe room air and the reappearance of signal intensity when the subject exhaled. The subject reported that he needed to swallow near the end of the dynamic imaging procedure, and it is interesting to note that a small area of high signal intensity appeared in the region of the stomach, consistent with some gas being transported to the stomach during swallowing.

Thin-section imaging.—The thin-section images exhibited the expected higher anatomic resolution that was seen in the depiction of the cartilage around the trachea and of the dark regions in the lung, corresponding to blood vessels. The images were noisier than the previous examinations, but the value was consistent with use of the larger flip angle, wider bandwidth, and thinner sections. The lower S/N for the second-pass sections was attributed to mixing of the already imaged He-3 gas (depleted magnetization) from the first-pass sections with the gas in the second-pass sections during the 15 seconds between passes; this mixing would lead to approximately a 30% reduction. Additional loss mechanisms likely resulted from a section profile that was somewhat wider than the section spacing. This indicates that sequential rather than alternate section acquisition would provide improved results. Finally, it is possible that the

second subject inhaled a smaller quantity of the gas, resulting in lower signal intensity than expected. He also may have loaded the surface coil differently than the first subject, leading to increased noise.

Other technical considerations.—Subjects reported no difficulty breathing the He-3 beyond one mention of dryness in the throat. The gas had no water vapor because of the processing, and so throat dryness was to be expected. Because the use of He-4 is well established in diving mixtures, the safety of He-3, which is chemically identical to He-4, should not be an issue. Subject comfort may be improved by adding water vapor or, for continuous breathing, mixing the He-3 with O₂ that is sufficiently moist before the gas is delivered to the subject.

The use of a transmit-receive surface coil with a large area worked well in this experiment, although the shape and size of the coil could be improved to provide better image uniformity and coverage. The posterior regions in particular suffered S/N loss due to the distance from the surface coil. This loss was a problem in terms of visualization and relative quantitation, because it was difficult to know whether the low signal intensity of a region was due to coil nonuniformity or poor ventilation. Of course, use of a small flip angle helped create a larger region of uniform excitation and reception than would result with use of a large flip angle (the magnetization close to the coil would disappear too rapidly with a large flip angle) (5). In future experiments, we believe development of a larger area “wrap-around” surface coil with a transmit-receive configuration would be valuable.

Radio-frequency power-level calibration also worked well with our procedures but may be too time-consuming for clinical application. If larger quantities of gas were available, preimaging could be automated to occur during a short preliminary hyperpolarized He-3 breath hold, while the steady reduction in signal intensity due to repeated excitations was observed. The rate of reduction would be used to calculate the flip angle. For single-pass imaging, the pulse sequence could include a slowly increasing flip angle calculated to keep the transverse magnetization constant during image acquisition. For dynamic image acquisition, however, use of much smaller flip angles would be necessary to preserve the magnetization throughout multiple acquisitions.

Interpretation of He-3 images.—The images obtained showed that the He-3 gas appeared to rapidly fill all lung spaces and was contained within the lungs, confined by the pleural boundaries of the lung and the trachea. There ap-

peared to be no visible He-3 signal intensity from the blood, the surrounding fat and muscle, or the mediastinal regions. Initially, He-3 was channeled into the lung air spaces in the same manner as a normal air mixture. During a breath hold, the He-3 subsequently moved by convection and diffusion. It is uncertain, however, how well the He-3 was confined to a given region, because He-3 is known to diffuse much more rapidly than air.

The diffusion coefficient of He-3 is on the order of $2.0 \text{ cm}^2/\text{sec}$ (7); hence, He-3 may move on the order of 1 mm in the 5 msec between phase encoding and read-out of the signal. Thus, the ultimate level of spatial resolution may be on the order of 0.5–1.0 mm for He-3. This would still be much higher resolution than is achieved in typical nuclear medicine images. In any case, the images are very promising for thin-section evaluation of ventilation at a segmental level and possibly for quantitation of the gas flow dynamics at a subsegmental level. Much work remains to be done, however, in the evaluation of differences in flow dynamics between He-3 gas-air mixtures and normal air before this technique is clinically applicable.

Although the S/Ns were good, higher values would allow thinner sections to be used. These higher values may be possible if larger quantities of gas are available so that the subject can

continuously breathe a mixture of He-3 and O_2 . Deep-sea divers routinely breathe a mixture of 16%–20% O_2 with the balance being He-4. Similar mixtures could be prepared for longer term imaging to create high-resolution images with good S/N.

Cost also must be considered in the evaluation of all new imaging methods. Presently, He-3 can be obtained for about \$120 per liter. This price is comparable to the usual cost of MR imaging contrast agents and may decrease if demand increases. The source of He-3 is tritium decay; thus its supply depends on the amount of tritium produced. The worldwide supply is limited but is probably sufficient for medical use. It would be possible in a commercial system to recover the He-3 and purify and recycle it, which would extend the supply considerably. The results of this study indicate that lung ventilation images with good resolution can be achieved with use of He-3. Future studies should concentrate on whether such images can contribute important information to the evaluation of lung and airway disease that would justify the cost of MR imaging at the frequencies of both H-1 and He-3. ■

Acknowledgments: We are grateful to Michael J. Souza for construction of the polarization chambers; Steve Suddarth, MS, for help with the preamplifier and coil construction; and Lucy Upchurch for pulse-sequence modifications. We also acknowledge valuable discussions with H. Dirk Sostman, MD, and Vic Tapson, MD.

References

1. Albert M, Cates G, Driehuis B, et al. Biological magnetic resonance imaging using laser-polarized ^{129}Xe . *Nature* 1994; 370:199–201.
2. Middleton H, Black RD, Saam B, et al. MR imaging with hyperpolarized ^3He gas. *Magn Reson Med* 1995; 33:271–275.
3. Happer W, Miron E, Schaefer S, Schreiber D, Van Wijngaarden W, Zeng A. Polarization of the nuclear spins of noble gas atoms by spin exchange with optically pumped alkali metal atoms. *Phys Rev* 1984; 29(suppl A):3092–3110.
4. Fukushima E, Roeder S. Experimental pulse NMR: a nuts and bolts approach. Reading, Mass: Addison-Wesley, 1981.
5. Evelhoch J, Crawley M, Ackerman J. Signal-to-noise optimization and observed volume localization with circular surface coils. *J Magn Reson* 1984; 56:110–124.
6. Kaufman L, Kramer D, Crooks L, Ortendahl D. Measuring signal-to-noise ratios in MR imaging. *Radiology* 1989; 173:265–267.
7. Barbe R, Leduc M, Laloe F. Resonance magnetique en champ de radiofrequence inhomogene. *J Phys* 1974; 35:935.